Catalysis Today 169 (2011) 156–166

Contents lists available at ScienceDirect

Catalysis Today

journal homepage: www.elsevier.com/locate/cattod

Retro-analysis of silicate aggregation in pentasil zeolite formation

B.M. Szyja*, E.J.M. Hensen, R.A. van Santen

Schuit Institute of Catalysis, Department of Chemical Engineering and Chemistry, Eindhoven University of Technology, Den Dolech 2, 5612AZ Eindhoven, The Netherlands

ARTICLE INFO

Article history:
Available online 21 September 2010

Keywords:
Zeolite synthesis
Nanoparticle
Silica precursor
Structure directing agent
Molecular Dynamics

ABSTRACT

We present a retro-analysis of the zeolite assembly process by the decomposition of the frameworks of MFI and MEL type zeolites. We propose structures of the building units and the intermediates of the increasing complexity and the corresponding reactions that are necessary to accomplish the assembly process. The proposed intermediate structures are consistent with mechanistic synthesis proposals, especially that of the Leuven group. Based on Molecular Dynamics simulations of key elementary reaction steps we analyze the interaction between the structure directing agents (SDAs) and the silicate precursor species in MFI and MEL synthesis. A key result is the necessity of the alkyl chains of the alkylammonium ion templates to stabilize cavities in intermediate silicate oligomers as well as their role to assist the aggregation of such silicate clusters to form channel intersections. In the process the SDA cations move to positions different from their original position before aggregation. The differences between the stabilizing effects of the quaternary propylammonium cation in the formation of the MFI structure vs. that of the quaternary butylammonium used in the case of MEL crystallization suggest that this interaction plays an important role in the synthesis process.

1. Introduction

The hydrothermal synthesis of zeolites has been widely explored [1–5]. The zeolite topology as well as its composition depends on many parameters such as the use of cations and specifically that of structure directing organic agents, the pH, the silica-to-alumina ratio as well as temperature and pressure. These factors have been widely explored, mainly because of the desire to discover zeolites of varying pore dimension [6,7] and stability [8].

Yang and Navrotsky [9] observed that there are two opposing trends in crystal growth chemistry. As silicate nanostructures tend to repel each other due to their negative surface charge lowering of the pH is desirable. On the other hand, formation of Si–O–Si bonds is base catalyzed, which makes it necessary to work at high pH. A breakthrough discovery was the use of organic cations and especially that of quaternary ammonium ions as structure directing agents. Their use as basic cations in zeolite synthesis [10–12] made possible the syntheses of high-silica zeolites. Moreover, as different structure directing agents result in a variety of structures, this provides a versatile method to discover new microporous crystalline zeolite materials of which the pentasil structures are most extensively used in the chemical and refining industry.

Within the pentasil family three structures are closely related. These are the MFI, MEL and FER structures, which are distinguished by the way channels connect the different cavities (Fig. 1). Whereas in the MFI structure zig-zag channels connect the cavities in the pentasil plane, the corresponding channels are linear in MEL and connect through the double-five rings. In FER the in plane channel has a 90 degree rotation compared to that of MEL and connects through the eight-membered rings. As a consequence, FER behaves in many catalytic reactions as if its channel structure was one-dimensional.

There are many propositions about the mechanism of zeolite formation. At the center stage of this discussion are the nanoscale intermediates that give rise to particular zeolite structures (for a detailed description see the review paper of Cundy and Cox [13]). Most important are the lock-and-key models, described in the early 1980s [14,15] and intensively explored by Thomas and co-workers [16,17], who proposed that the fit of the shape and the volume of the structure directing organic cation with the shape and the volume of the zeolite cavity is the controlling parameter in zeolite synthesis. This model implies an in essence thermodynamic view. The size and charge of the positively charged cations compensate the negative charge of the zeolite framework due to the presence of three- or lower-valent cations incorporated in the siliceous zeolite framework. The match of shape and volume drives water out of the cavities and stabilizes the zeolite [18], although recent evidence suggest that water might play supporting role in stabilizing different parts of the framework [19,20].

Careful analysis of colloidal silicate–TPA structures performed by Ravishankar et al. [21] resulted in the finding that the TPA cation is present in two different environments within the MFI structure,

* Corresponding author. Tel.: +31 40 247 2124.
E-mail address: b.m.szyja@tue.nl (B.M. Szyja).

0920-5861/$ – see front matter © 2010 Elsevier B.V. All rights reserved.
doi:10.1016/j.cattod.2010.08.018

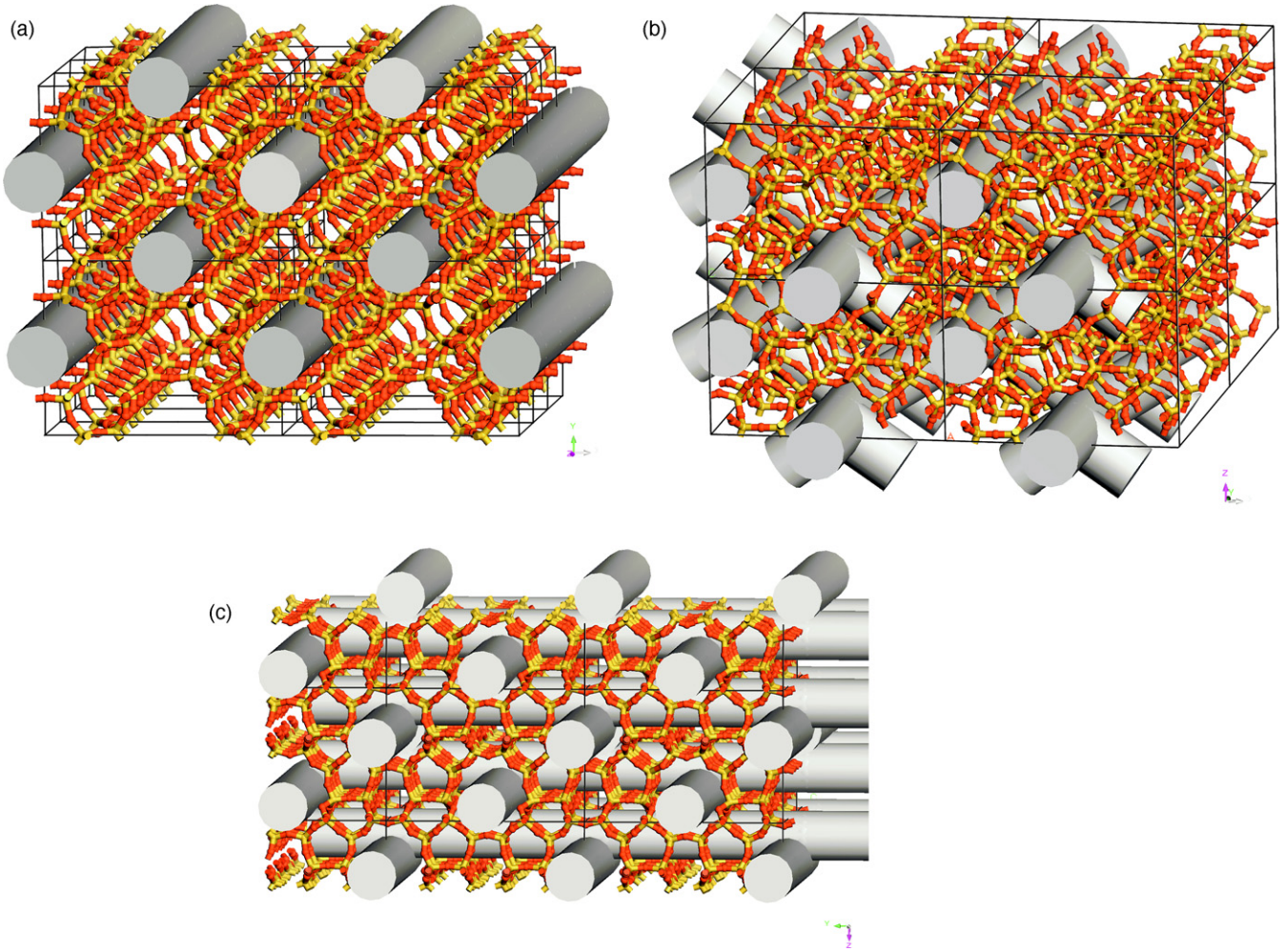

Fig. 1. The different channel directions in FER (a), MFI (b) and MEL (c) framework topologies (indicated by grey tubes). The channels in FER are parallel to each other and do not intersect, MFI has two types of channels, i.e. straight and zig-zag ones and MEL has only straight channels that cross perpendicularly.

that is at the channel intersections and at the external surface of the growing crystals. Cundy et al. [22] suggested that the stabilizing role of this latter type of TPA ions originates from preventing aggregation upon collisions of the colloidal structures. In an aqueous environment, the zeolite crystals have a negatively charged surface. The positively charged TPA ions will align themselves on the particle surface, thereby creating an electric double-layer. This is also related to the other role of tetraalkylammonium cations, in early step of synthesis: at first, the template is considered to form the micelle-type nanoparticles, what results in differences of aggregation of nanoparticles with respect to the free solution [23].

Another important factor is entropic stabilization in zeolite precursor complexes such as encountered in dense clatrate-type systems that are formed with symmetric template molecules. Their stability is mainly due to the entropy of the rotation of the template molecules [24]. The formation of siliceous sodalite, the structure of which results in free rotation of the tetramethylammonium cation, is a very well-known example of such entropic stabilization.

For particular systems the molecular chemistry of zeolite synthesis has been studied in detail. For faujasite type systems, Jacobs and co-workers [25] proposed that initially formed four-, five- or six-membered (alumino)silicate rings aggregate into layers. The fusion of parallel layers, oriented slightly different with respect to each other gives rise to different zeolite structures related to the faujasite family. Three reaction steps are essential, i.e. (i) (alumino)silicate ring formation, (ii) aggregation into larger molecular defined complexes and (iii) fusion of these complexes into the three-dimensional structure of the zeolite. Similarly, Ozin and co-workers [26] interpreted formation of different zeolite-resembling structures in $AlPO_4$ systems. After initial ring formation, the even-membered rings, order into strings. The organic cations act as templates directing different assemblies of the strings, resulting in different structures. The Leuven group [27,28] proposed an alternative model of silicalite synthesis, which is not based on the formation of layered or string-type connected silicate ring systems, but instead on intermediate formation of anionic molecular clusters containing 33 Si atoms (Si_{33}). Such clusters can be considered the result of the associative reaction of three Si_{11} clusters [29], which in turn can be considered as three condensed five-membered silicate rings. Note: add part about the mixture of many different silica species. Template will preferentially stabilize particular intermediates. Key structure parameters that can control silica–silica interactions.

We discussed in a previous paper the formation of Si_{22} oligomers from Si_{11} oligomers assisted by hydrophobic stabilization by the alkyl chain of a quaternary propylammonium ion [18]. In this aggregation step there is no essential difference in the stabilizing role of the quaternary ions with side chains of different lengths. Herein we will explore by computational methods the discriminating effect of the use of *n*-propylammonium and *n*-butylammonium cations to form respectively the MFI and MEL structures in subsequent stage of synthesis.

What these models have in common is that zeolite formation proceeds by incorporation of pre-organized molecular entities into the growing zeolite crystal. No definitive proof of this is yet available and we discuss this issue later. In this context, the AFM experiments of the Anderson group [30,31] are of interest. They interpret growth of zeolitic crystal surfaces in terms of the attachment of definite silicate clusters.

The question of growth through attachment of monomers and clusters is complex to settle because of the fast exchange between silicate monomers and silicate units in ring systems, compared to the time scales of zeolite precursor formation [32,33].

Whereas the above zeolite structure models involve molecularly defined intermediates, zeolite synthesis usually occurs from transformations in a highly disordered gel phase. Especially studies of silicalite (MFI) formation in solution phase [23,34,35] have shown that in the prenucleation phase nanosized intermediates are formed. They have colloidal hydrogel type properties and their possible (partial) structure is subject to major disputes (see the review paper of Cundy and Cox [13] and the references therein). The nanosized particles possibly are part of the earlier defined step (iii), where the transformation from highly disordered locally ordered molecular identities give the nucleating particles that result in crystal growth. A recent paper by Tsapatsis and co-workers [36] suggests that the hydrogel nanoparticles slowly transform into zeolite precursors by interpenetrating base template molecules.

When zeolite synthesis is considered to be kinetically controlled, one has to distinguish at least the three separate reaction steps and the selectivity to form a particular intermediate complex. The key to the formation of the final structure may be in principle determined by one of the three steps or a combination of them.

There are many examples in the literature, for instance the successive formation of different zeolite phases in one reaction mixture as a function of time, that indicate that zeolite formation is predominantly controlled by kinetic factors, to which the relative stability of reaction intermediates is relevant [13].

1.1. Aim and scope of this work

In this paper we explore at which stage of the synthesis the structure directing agents discriminate between the two pentasil structures MFI and MEL (we are assuming for the clarity, that TBA leads exclusively for the formation of MEL framework, while in reality usually the intergrowths are observed, and obtaining pure MEL structure requires more strict synthesis control). We will present results of Molecular Dynamics simulations of the association of the Si_{33} units as proposed by Kirschhock et al. for MFI and MEL and compare these with the relative stabilization of the final siliceous structures by the respective templates. The interpretation of such simulations is only useful if a consistent overall scheme is provided for the formation of the final structures based on the association of intermediates of increasing complexity. Therefore, we will provide

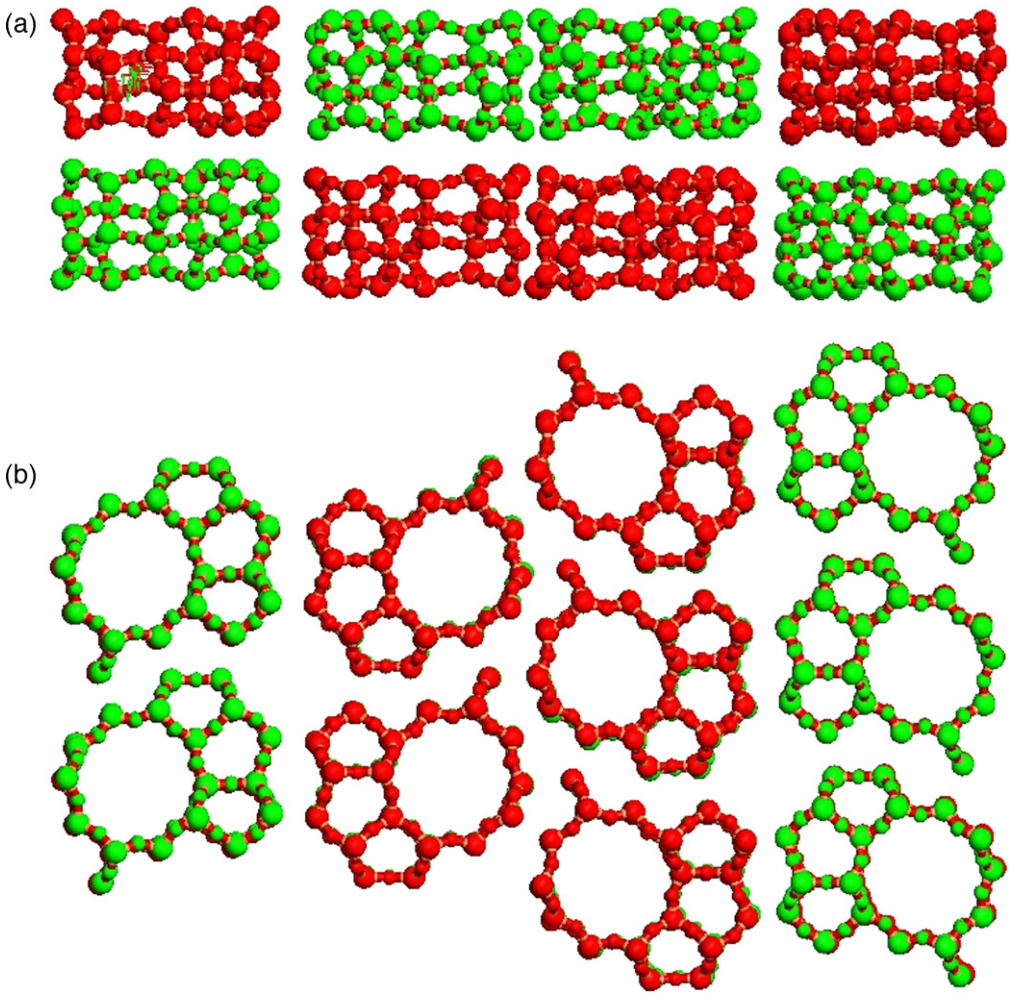

Fig. 2. Decomposition of the MFI structure shown in two directional views along the [0 0 1] (a) and [1 0 0] (b) directions. R- and L-Si_{33} precursors are shown in green and red color respectively. (For interpretation of the references to colour in this figure legend, the reader is referred to the web version of the article.)

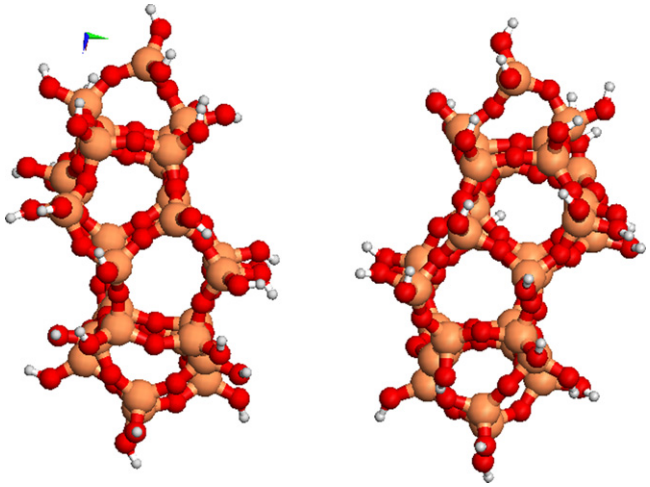

Fig. 3. Two enantiomeric forms of the MFI-Si_{33} building unit used to deconstruct the MFI structure.

an in depth analysis of the intermediate path towards the pentasil structures. Interestingly, it will turn out that in order to complete the structure, not only the aggregation of particular oligomers has to be considered, but also in different stages of agglomeration, additional monomers will have to be incorporated.

2. Results and discussion

2.1. Retro-analysis of the building units of the pentasil structures

The retro-analysis deconstruction of the zeolite structure can be done in different ways. We follow here the leads from the Leuven group [27] that postulated that a Si_{33} oligomeric species containing a cavity is the essential building unit for consecutive zeolite framework formation. Fig. 2 illustrates the decomposition of the MFI structure into these building units. The deconstruction of the MFI structure requires two enantiomeric Si_{33} clusters. Side views of these Si_{33} clusters are given in Fig. 3. The R- and L-Si_{33} precursors alternate, when moving along the *y*-direction of fully formed MFI crystal, so that after a R-building unit comes a L-building unit, and so forth. The same applies in the *x*-direction, except they are now alternative every two units. In this direction, the Si_{33} precursors are arranged in an RRLLRRLL pattern.

A possible sequence of the MFI assembly process starting from the two enantiomeric Si_{33} clusters and containing the TPA cationic template molecules is shown in Fig. 4. Next, we will present simulations of the interaction of these cationic ions with the Si_{33} units. It is useful to remember the results of our earlier studies [20,29], which demonstrated the importance of the interaction between the organic cation and the MFI-Si_{33} unit. Only when one of the propyl branches of the organic cation inserts into the open center of the Si_{33} unit, this fragment is stable. Otherwise, the structure collapses by contraction of the atoms towards the center of the channel. These results were based on quantum-chemical simulations in the gas phase and classical Molecular Dynamics simulations in the liquid phase.

The quaternary ammonium cations are too large to be fully accommodated in the Si_{33} cavity. As demonstrated earlier [18], the organic cations also play a role in bringing the building units of the Si_{33} clusters together. To facilitate this process, the organic cations have to be located between the aggregating oligomers. The cations are then partially pushed out of the cavity upon the formation of initial channel, so that only one alkyl group is pointing to the center of the channel.

Interestingly, REDOR NMR experiments [37] noted a discrepancy between the measured effective larger distances between the TPA cation and Si in Si_{33} precursor mixtures and predictions of model calculations of TPA in the Si_{33} oligomer. This difference can now be interpreted as the partial displacement of the template out of the Si_{33} cavity.

Fig. 4 also shows two different modes of assembly of the two Si_{33} units, that is the formation of a straight MFI channel (top part) and aggregation in the second and third dimensions (bottom part). In order to complete the structure, new template molecules have to be incorporated in between four Si_{33} units along the linear channel. Once these four Si_{33} units have aggregated, different forces drive the aggregation of larger units in the next building step. An important observation is that the "ghost" channel that is formed in this step has exactly the same geometry as "normal" channels that were formed beforehand. The location of the silicon and oxygen atoms belonging to four Si_{33} precursors necessary to obtain this channel is equivalent to those from each of the precursors.

In summary, our analysis implies that once the Si_{33} units combine into linear channels and concomitantly loose their enantiomeric properties – as a consequence of the fact that two enantiomeric units are incorporated simultaneously – they follow at least two steps: (i) incorporation of two additional template molecules to recombine at least eight Si_{33} units and (ii) agglomera-

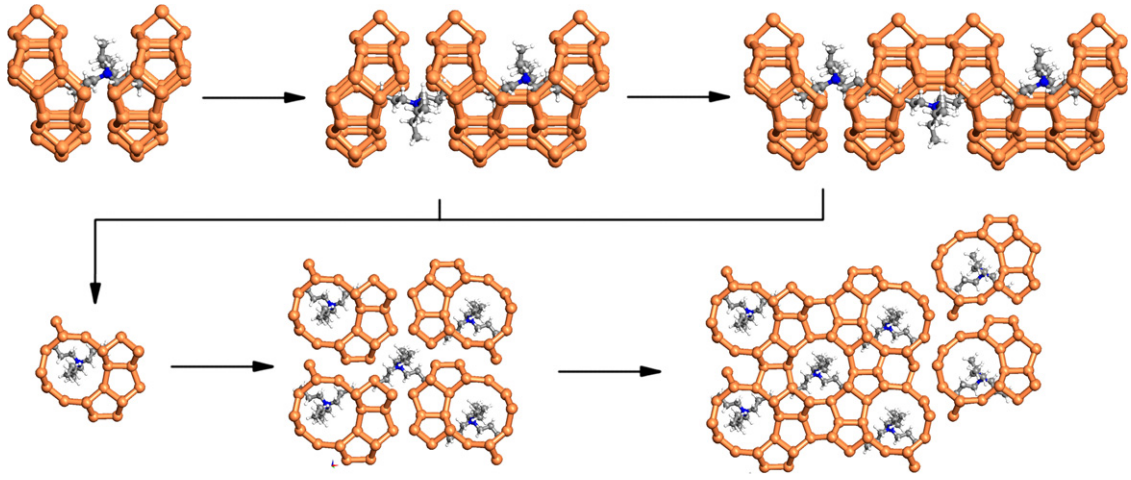

Fig. 4. Proposed sequence of the assembly process of the MFI structure from TPA-Si_{33} units.

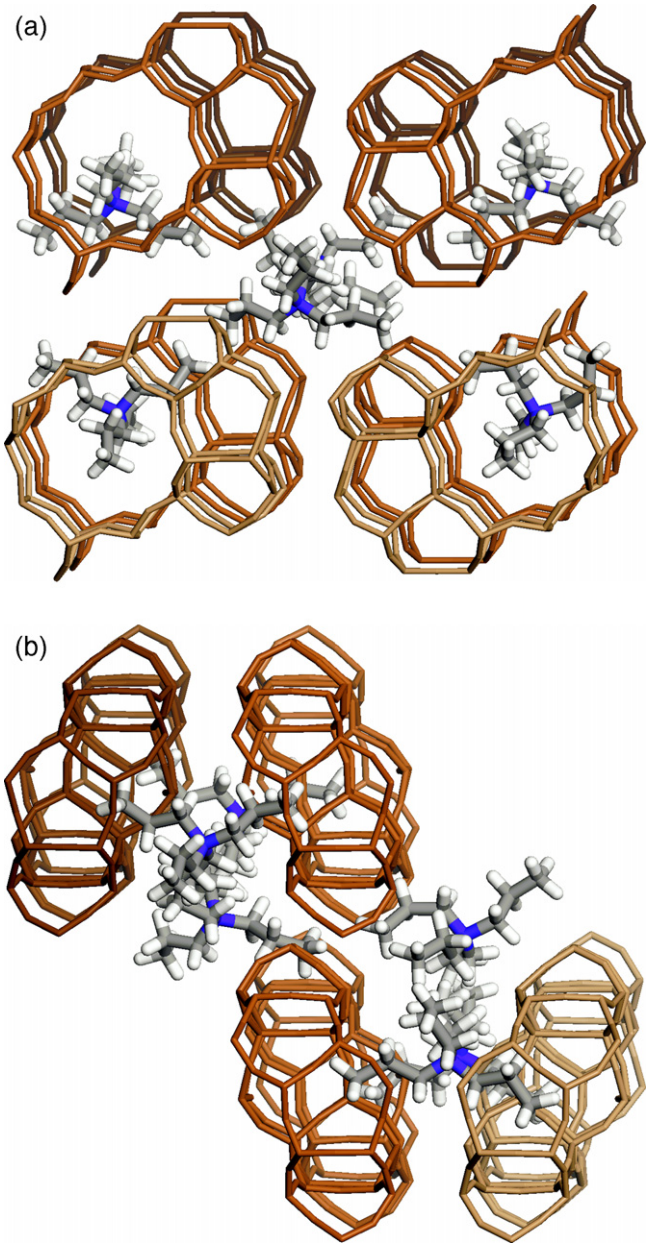

Fig. 5. The formation of MEL from 8 MEL-Si_{33} units: front view (a) and side view (b).

tion of these nanoparticles, which requires a different mechanism of growth, since there is no room for another SDA between them.

These eight Si_{33} precursors are required to form stable nanoparticle, because the zig-zag channels in the MFI structure alternate. That is, when viewing along the straight pore direction, one first encounters an intersection with a zig-zag channel such that the latter channel points downwards. The following intersection has the zig-zag channel pointing upwards (Fig. 1b). A unit consisting of eight Si_{33} precursors is shown in Fig. 5. The precursors shown in the top line are shifted instead of being aligned straight above the bottom precursors. This structure is preferred over the more compact one, in which the precursors are not shifted. In the latter structure, access to the pore center by other species existing in the solution would be blocked, bringing problems to the incorporation of monomeric silica.

The size of the structures based on eight MFI-Si_{33} unit is 2.5–3.0 nm, which is similar to that of disordered nanoparticles identified as the prenucleation clusters in silicalite-1 synthesis [38]. Note the low value of the template over Si atom ratio of 6/264. Tsapatsis and co-workers [36] have suggested similar intermediate particle sizes in their silicalite formation studies. In the final step the eight MFI-Si_{33} units have to aggregate further. This step involves bond-forming reactions between the oligomeric clusters, which do not require templating action.

If we accept the view that the prenucleation nanoparticles are the aggregates of eight Si_{33} units, which are still in the hydrogel stage and which require time to properly order to allow further aggregation through Si–O–Si bond formation, one can identify two criteria for their relative stability. Firstly, for further growth into two dimensions organic cations have to be removed from in between the ring systems. This is an activated process. The Si–O–Si ring systems of the Si_{33} units are hydrophobic and strongly interact with the hydrophobic tetrapropylammonium cations [39]. Secondly, continued zeolite crystal nucleation requires the incorporation of additional monomeric silicate species, since the Si_{33} units do not provide all the Si atoms present in the MFI framework. Per Si_{33} unit three silicate monomers have to be incorporated. These missing atom positions are indicated in Fig. 6.

The structural principles to deconstruct the MFI structure can also be employed to deconstruct the other pentasil structures. The deconstruction of the MEL structure is shown in Fig. 7.

Similar to the MFI case, “ghost” channels are present between already assembled precursors. It is important to stress again that the geometry of this channel is exactly the same as that of the channels already formed in Si_{33} precursors by assembly of the Si_{11} oligomers. With respect to the alignment of the enantiomers, the same rules apply as for the MFI case. Along the [0 1 0] direction, the R- and L-enantiomers are alternating, while along the [1 0 0] direction they are alternating in a RRLLRRLL pattern. Note that, whereas the close analogy with the decomposition for the MFI structure is obvious, the detailed structure of the Si_{33} structure to build up the MEL topology is different. The subtle difference in the construction of the MEL structure is apparent from Fig. 8.

Similar to Fig. 4, this figure shows the side-on view of the formation of a straight channel made up from enantiomeric MEL-Si_{33} intermediates. Contrary to MFI, the MEL structure has channels that cross perpendicularly. Consequently, MEL has two types of channel intersections [40]. The first one (MEL(I) according to the De Vos Burchart nomenclature) is shown as the top left connection in Fig. 8. Two MEL-Si_{33} units connect their most planar surfaces to form a small part of the intersecting channel. The other MEL(II) type forms when the MEL-Si_{33} precursors only connect their tips, which forms the large part of the intersection. Fig. 9 also shows the agglomeration of columns of MEL-Si_{33} oligomers to form the three-dimensional structure. As for MFI, an extra organic cation has to be inserted between four aggregating columns and aggregation of eight MEL-Si_{33} clusters leads to channel cross-section formation (Fig. 9). One should be aware that, contrary to the conclusions of de Vos Burchart, all intersections in Fig. 9 are occupied by the organic cations. Their paper claims that only 2.4 out of 4 intersections are occupied by the tetrabutylammonium cations. This issue will be discussed in more detail below. Again the final MEL structure is only formed if missing atoms complement the final formation (Fig. 10).

2.2. Simulation of MFI-Si_{33} and MEL-Si_{33} aggregation

As pointed out in the introduction, the type of organic cation may play a discriminating role in directing the formation of MFI-Si_{33} vs. MEL-Si_{33} units out of three Si_{11} oligomers, direct the binary assembly of Si_{33} units and/or form the zeolite cavities by occupying the intersections.

Before discussing the aggregation of the Si_{33} building units we shortly summarize reaction paths that lead to the different Si_{33}

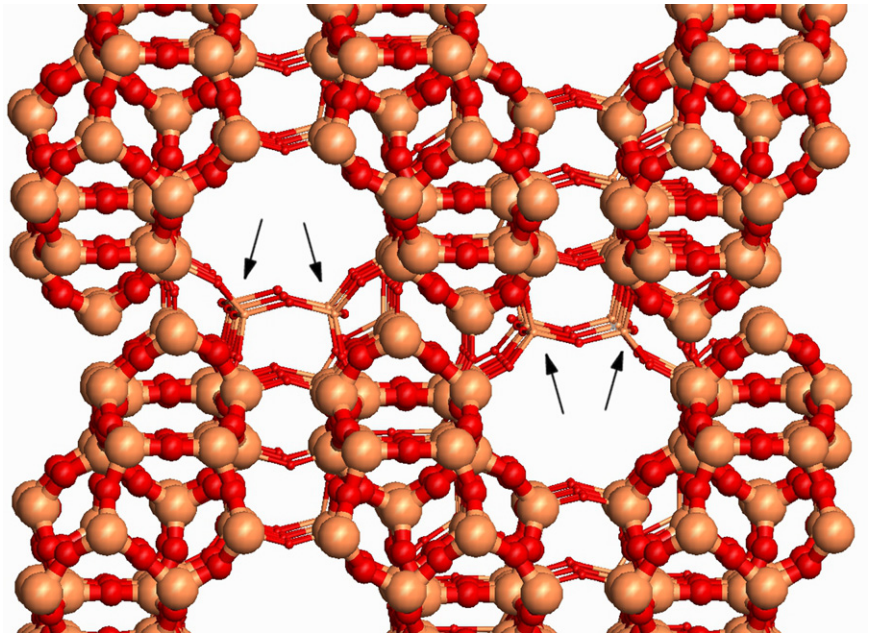

Fig. 6. The extra Si and O atoms required to complete the MFI structure, which do not belong to Si_{33} units (missing atoms shown as small spheres; atoms belonging to precursors shown as large spheres (red: oxygen, light brown: Si). (For interpretation of the references to colour in this figure legend, the reader is referred to the web version of the article.)

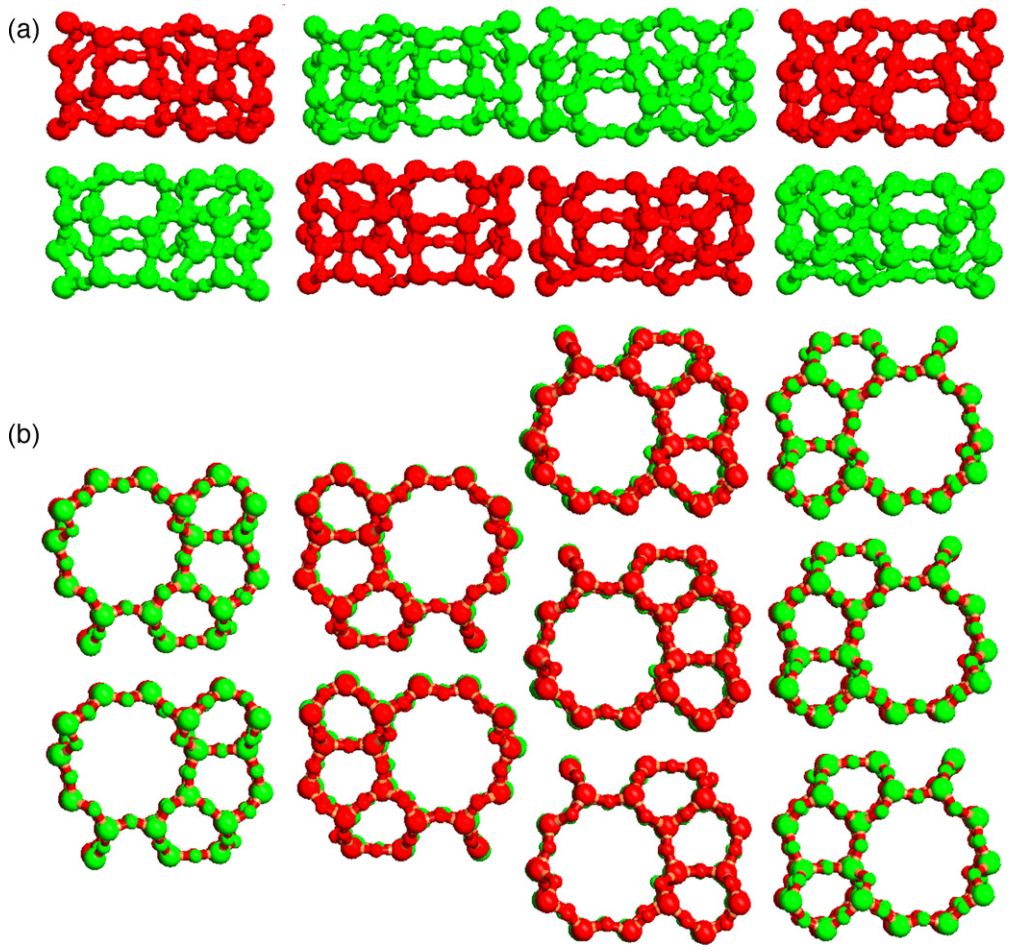

Fig. 7. Decomposition of the MEL structure: R- and L-Si_{33} precursors are shown in green and red color respectively. (For interpretation of the references to colour in this figure legend, the reader is referred to the web version of the article.)

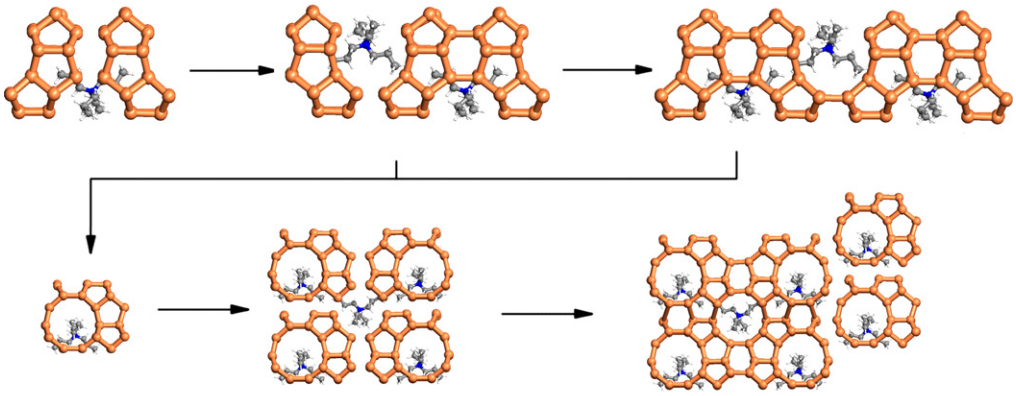

Fig. 8. The construction of MEL with the positions of TBA templates. Note the difference in interconnection between precursors in the top line, which is the cause of formation of two types of channel intersections.

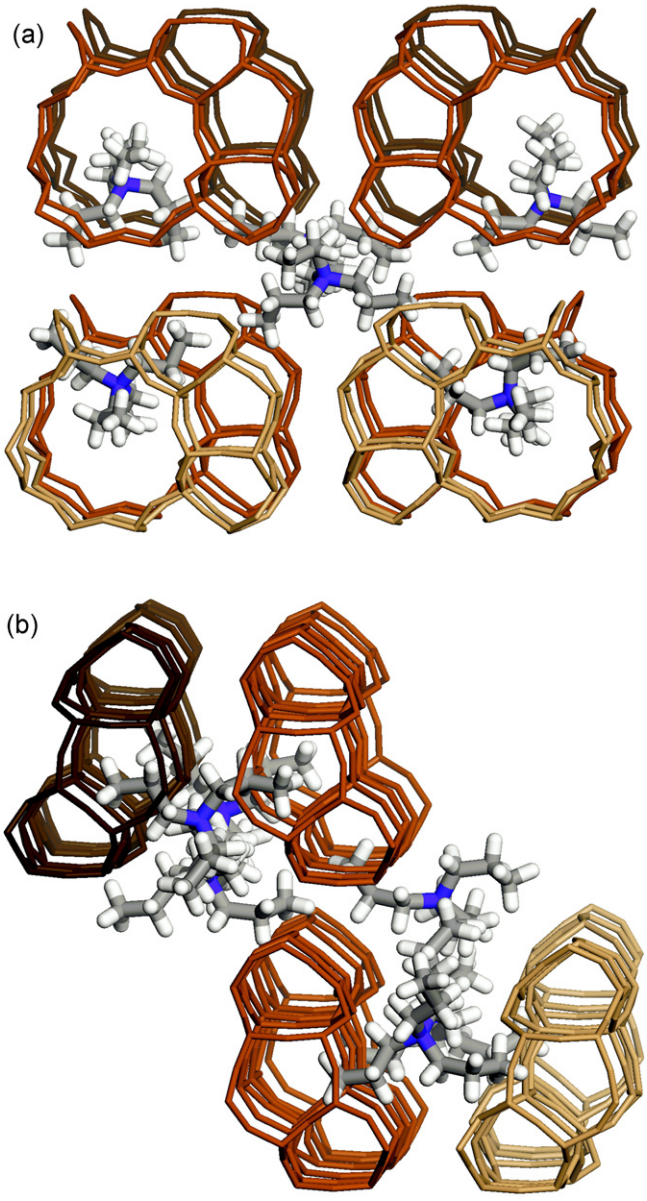

Fig. 9. The formation of MEL from 8 MEL-Si_{33} units: front view (a) and side view (b).

building units of the respecting MFI and MEL structures. This is illustrated in Fig. 11. An intermediate step in the formation of Si_{33} units is the formation of a Si_{22} oligomer. We shall base its formation on the association of Si_{11} sheet-like oligomers that are built up from three five-membered rings. As indicated in Fig. 11 the formation of MFI-Si_{33} vs. MEL-Si_{33} in essence implies the choice between Si_{22}-controlled reaction paths with intermediates that contain different ratios of five- and six-membered rings. Using Molecular Dynamics simulations we analyzed previously the formation of the Si_{22} units from Si_{11} units for the MFI system [18].

Computational studies on the relative stability of smaller ring systems, that are intermediate to Si_{11} formation, have been done extensively in the Catlow group [41]. They report differences in the relative stability of particular oligomers in contact with different quaternary ammonium cations.

Many of the intermediates that we discuss rapidly exchange with monomers from solution [33]. This implies that when one intermediate or the final product is relatively stable compared to the other intermediates, the overall concentration of intermediates can rapidly shift to that particular intermediate. For example, in case the MEL-Si_{33} intermediate is particularly stable when associated with tertiary butylammonium, all the intermediates of Fig. 11 may rapidly interconvert and the precursor MEL-Si_{33} dominates the selectivity of zeolite formation. We will revisit the interaction of alkylammonium ions with the smaller oligomers in another study.

Here we will discuss simulations of Si_{33} unit aggregation and compare the energies of the final MEL and MFI structures.

2.2.1. Computational method and modelling

Seven different systems have been studied. Since we are interested in the selective discrimination of MEL or MFI formation from the respective MEL-Si_{33} and MFI-Si_{33} oligomers we not only studied the TBA/MEL-Si_{33} (two types, as there are two types of channel intersections in MEL framework) and TPA/MFI-Si_{33} combinations, but also cross-simulations of TPA with MEL-Si_{33} (again two types) and TBA with MFI-Si_{33}. A reference simulation of TMA with MFI-Si_{33} has also been performed.

Each investigated system contained two Si_{33} units in contact with template ion. We have applied the periodic boundary conditions (PBC) around the molecules and filled the remaining space with water up to the desired density (1 g/ml) while imposing a cubic unit cell with constant size of 30 Å × 30 Å × 30 Å. It implies approximately 600 water molecules.

The CVFF forcefield [42,43] has been used in all Molecular Dynamics simulations. This forcefield have been developed for small organic molecules, but has been extended for materials

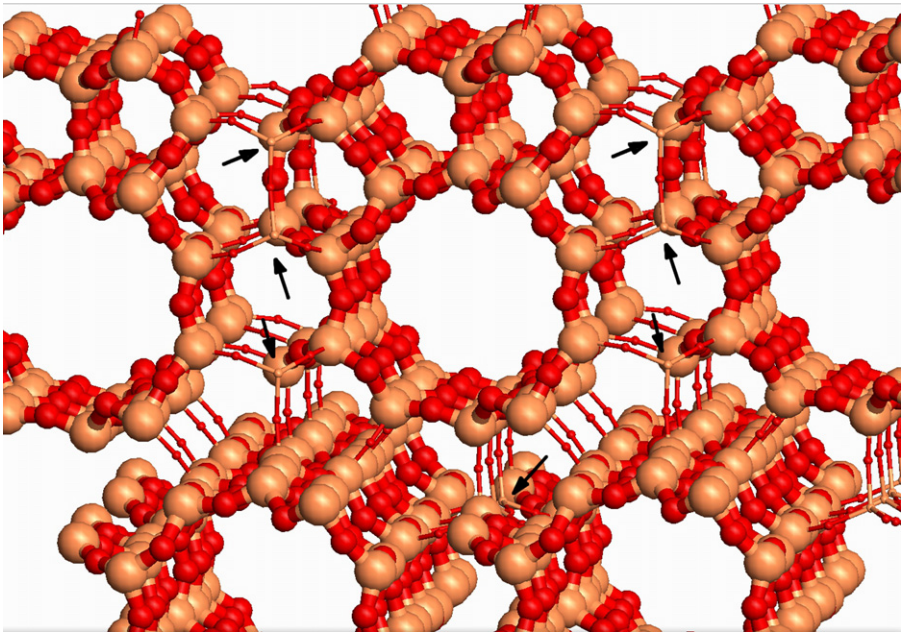

Fig. 10. The positions of the extra atoms needed to be incorporated into the MEL structure.

science applications including zeolites and related materials, for which it has been successfully applied [20,44–46]. The computational engine was Discover version 2008.2 included in Materials Studio version 4.4 by Accelrys Inc.

To this end, partial charges have been assigned to all atoms using an internal forcefield calculation procedure. The total charge of the system is zero and the precursors have been deprotonated in randomly selected –OH group in order to compensate the positive charge of the structure directing cations. As the calculations involved PBC, we have applied the Ewald summation method.

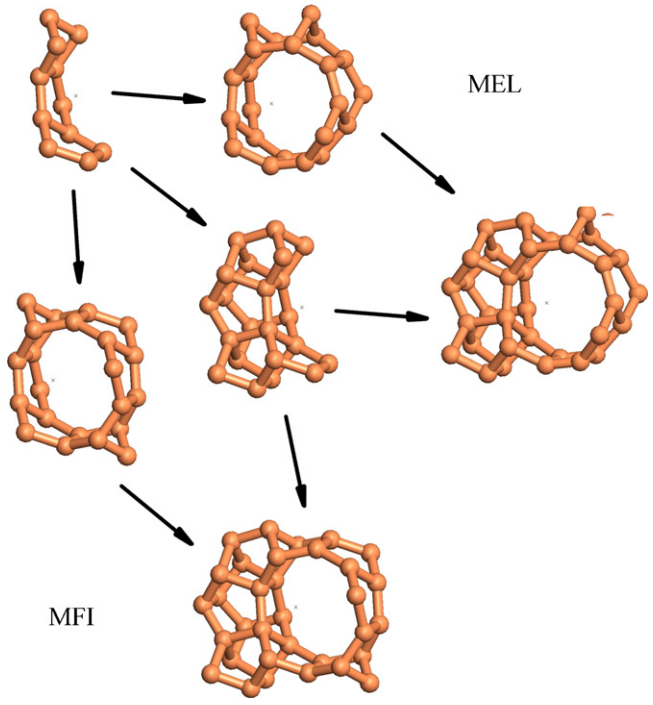

Fig. 11. The different Si_{33} formation paths: discrimination between MFI and MEL-Si_{33} building units.

We have chosen similar initial configuration for all models, as we wanted to avoid the issue of results diverging to a different local minimum. This point will be discussed in more detail in the results section. The initial geometry selected for this study can be best described as the tetraalkylammonium cation in between two Si_{33} precursors. The simulations have demonstrated, that it is indeed the most stable configuration, as in most cases the systems evolve to this configuration even from different starting points.

2.2.2. Analysis of Molecular Dynamics simulations

Fig. 12 illustrates the structures derived from the Molecular Dynamics runs. An important observation is the position of the tetraalkylammonium (TAA) ions. It is commonly found that the TAA cation is located in between the precursor Si_{33} species, with one alkyl group pointing towards the initial channel in the precursor. Depending on the distance between the Si_{33} precursors, other alkyl groups may also find enough room to fit into the cavity of the other Si_{33} precursor (Fig. 12b). In this way, a TAA cation aligns the cavities in such way that a channel is formed, because the cavities meet at one point. Moreover, the two remaining free alkyl groups can fit at the half-pipes of the intersecting channel. This behavior leads to the stabilization of the channel intersection and generally follows the lock-and-key scheme.

Our previous work has shown that the Si_{33} oligomer collapses when its cavity is not stabilized by interaction with an organic aliphatic chain. Simulations for TPA and TBA show that the initial channel retains its shape only when the alkyl group is located inside the cavity. On the contrary, the methyl groups of TMA are too short to penetrate the initial channel formed inside the precursor. Consequently, the TMA cation does not stay close to the initial channel and the structure of the Si_{33} precursor becomes greatly distorted, especially the fragment forming the surface of the channel. This is in agreement with our previous work [18].

Fig. 13 shows that the interaction of the TAA cation with the Si_{33} precursor differs between TBA and TPA. The distance between the nitrogen atom of the TAA ion and one of the Si atoms of the precursors (selected so that it was part of the “head” fragment, the geometry of which is common for both MFI- and MEL-Si_{33} precursors) is slightly smaller for the TBA/MEL(I)-Si_{33} case than for the TPA/MFI-Si_{33} one. This result implies that the TBA template

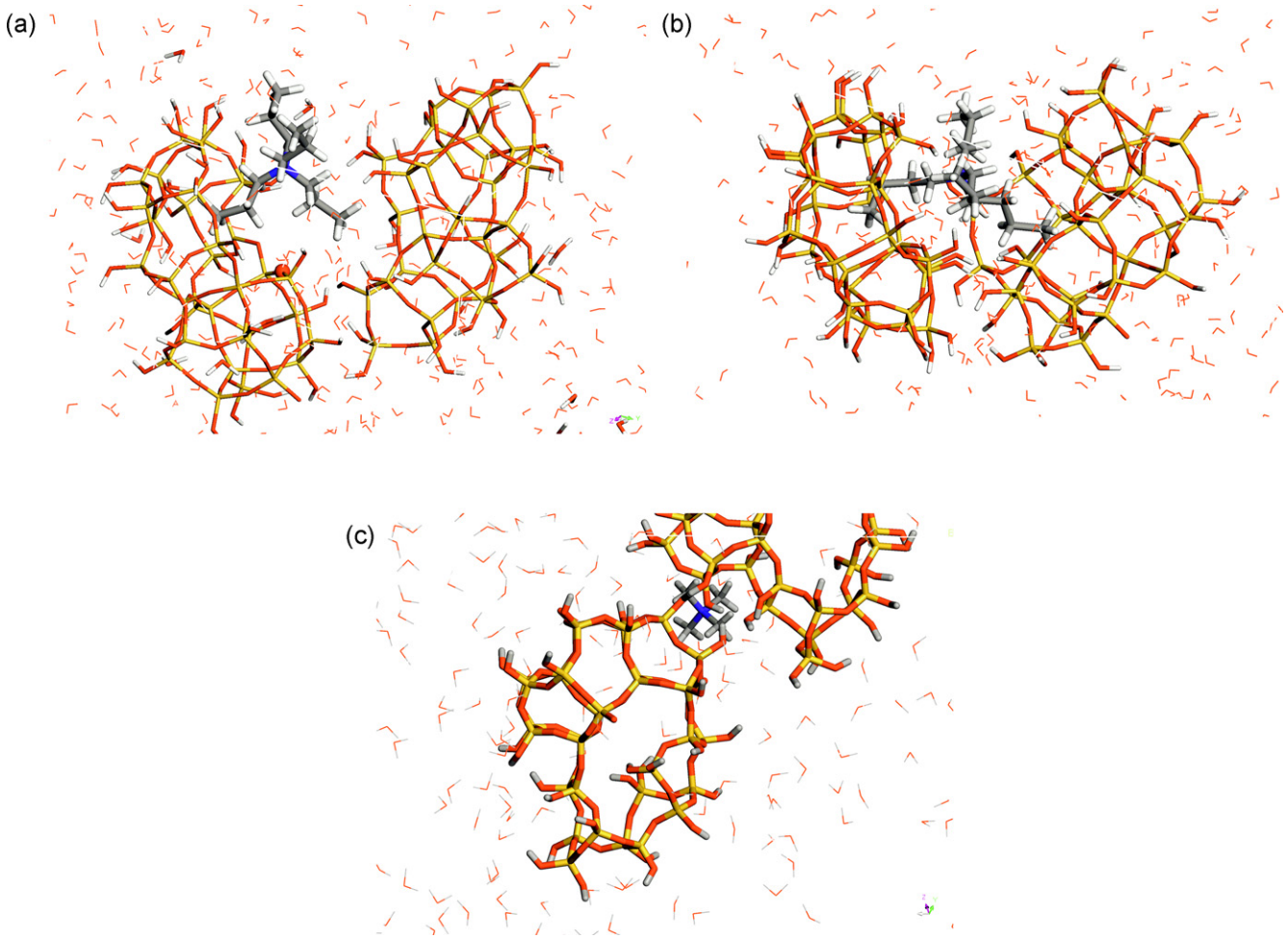

Fig. 12. Snapshots of MD simulations of (a) TPA/MFI-Si_{33}, (b) TBA/MEL-Si_{33} and (c) TMA/Si_{33} systems.

is located deeper in the cavity of the MEL(I) structure than is the TPA template in the cavity of the MFI structure. On the other hand, for the TBA/MEL(II)-Si_{33} system we can observe larger N–Si distance than for the TPA/MFI-Si_{33} and TBA/MEL(II)-Si_{33} systems. This observation together with the weaker interaction between SDA and MEL in this type of intersections found by de Vos Burchart [40] also supports the lock-and-key scheme. The molecules do not match geometrically as good and therefore do not interact as strong as in the TPA/MFI or TBA/MEL(I) systems. This observation can also explain the lower occupancy of the TBA in the MEL(II) site.

Interestingly, there seems to be another correlation between the distance and lower occupation of the intersections in MEL by the TBA cations. Intuitively, due to the longer chain of the butyl groups and the deeper location of butyl groups in the cavity, one proposes that each single butyl chain can possibly occupy both sides of the precursor's cavity and therefore prevent other TBA ions from having close contact with the same precursor. Our simulations show that other TPA molecules may occupy the same cavity from the other side, because the TPA molecules do not penetrate the cavity as much as TBA does in the MEL case. As shown in Fig. 9, every intersection is occupied by TBA cations, but only before the condensation of the precursors occurs. The role of TBA in the alignment of the channels in the proper way is therefore slightly limited.

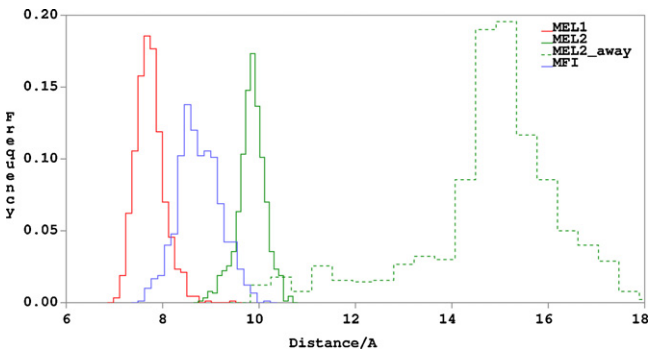

Fig. 13. The distance between the N atom in the template and a fixed Si atom of the Si_{33} precursor species for the various MD simulations.

In the TBA/MEL(II)-Si_{33} simulations we observed that the TBA cation moved away from its close proximity to the MEL-Si_{33} unit (Fig. 13). Although the starting point was very similar, the simulation diverged to different local minimum, which is the evidence, that at some point the transition was very easy to cross. Initially, the N–Si distance is equivalent to that of TPA–MFI (~8.5 Å), but subsequently the distance increases quickly to reach 14–16 Å in the next stages of the simulation. This corresponds well with the lower occupation of TBA in MEL(II) intersections.

For the TPA/MFI-Si_{33} system, we note a substantial decrease of the interaction energy which is already negative (interaction is becoming stronger) of about 15 kcal/mol between the template and the silicate oligomer during the simulation. This stabilization effect is due to the reorientation of the TPA molecule with respect to the Si_{33} unit. At the start of the simulation only one of the precursors is in close interaction with the TPA cation. Once the two oligomers pair with the TPA, they remain in close contact throughout the sim-

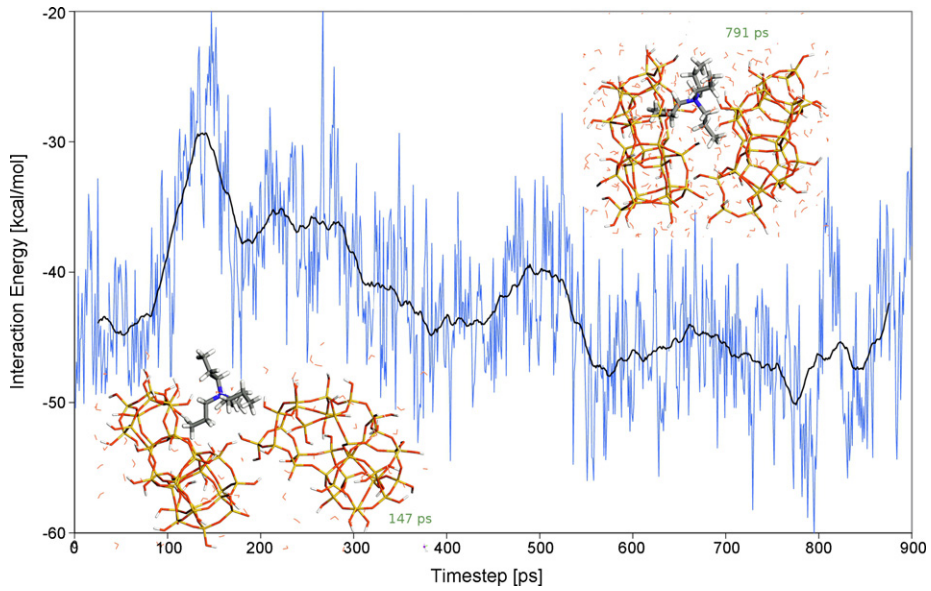

Fig. 14. The interaction energies between the TPA and MFI-Si_{33} precursors.

ulation and, concomitantly, the relative orientation between the TPA cation and the silicate precursors becomes more close to that in the final MFI crystal. The interaction energy as a function of the simulation time and two representative structures at simulation times of 147 ps and 791 ps are shown in Fig. 14.

The interaction energies during the simulation of the TBA/MEL-Si_{33} system are given in Fig. 15. The observation of a stronger interaction when the distance between TPA and Si_{33} becomes lower is valid here as well. What differs for the MEL and MFI cases is that the time to reach the close interaction between the various precursors is much longer in the TBA/MEL-Si_{33} system. TBA in MEL-Si_{33} is much less mobile and does not significantly evolve into more stable structure with stronger interaction. In consecutive runs, we have changed the initial configuration of the system in such way that the TBA is already in close contact with the MEL-Si_{33} oligomers. As there are two possible MEL-Si_{33} interconnections equivalent to the MEL(I) and MEL(II) intersections, we have carried the MD simulations for both such systems.

With the precursors apart, the simulation results in an interaction energy in the order of −20 kcal/mol. For the MEL(I) and MEL(II) type intersections, interaction energies amount to approximately −70 kcal/mol and −50 kcal/mol, respectively. These results are in agreement with the de Vos Burchart data, which also indicate differences in interaction energies for different intersections in fully formed crystals.

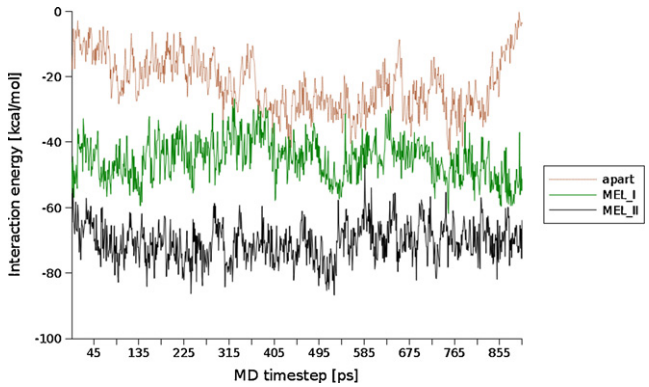

Fig. 15. The interaction energies between TBA and MEL-Si_{33} precursors.

In order to provide further evidence for the crucial role of the organic cations in this step of the zeolite formation mechanism, we have also carried out simulations of TPA with two MEL-Si_{33} precursors and TBA with two MFI-Si_{33} precursors. The results of all those simulations are collected in Table 1.

These results confirm the discussion given above. TPA stabilizes the MFI type intersection, whereas for the TBA the MEL(I) type intersection is the most stable configuration. For the MEL(I) type intersection, the difference in interaction energy is favored by 50 kcal/mol for TBA compared to TPA. This difference warrants the conclusion that the template TBA stabilizes the alignment of the precursors in the MEL geometry. One should also keep in mind, however, that the stabilization of a single intersection is not equivalent to the stabilization of the whole crystalline framework. The unit cell of the MEL crystal contains 4 intersections of channels ($2 \times$ MEL(I) and $2 \times$ MEL(II)). When occupied by TPA, the total interaction energy amounts to 107 kcal/mol. For the TBA case, only 2.4 intersections are occupied, most likely two of them residing in the MEL(I) configuration because of its higher stability compared to the MEL-II one and another 0.4 in the MEL(II) configuration with a weaker interaction between the template and the silicate framework. The total stabilization energy amounts to 159 kcal/mol. The difference is argued to be the controlling factor in this step of zeolite synthesis.

The key difference between TPA and TBA is the length of the hydrocarbon chains. Whereas TPA can occupy all intersections of MFI or MEL without experiencing detrimental repulsive interactions, this is not the case for TBA. Complete occupation of all channel intersections in MFI as well as MEL is not possible. Whereas isolated TBA has a stronger interaction with both lattices, it stabilizes to a limited extent because of this partial occupation. The preferential formation of MFI framework by TPA cation is due to its possibility to occupy all channel intersections. In this way, it overcomes the stabilization of TBA that only can occupy part of them.

Table 1
The average interaction energies (in kcal/mol) of the MFI, MEL(I) and MEL(II) systems with TBA and TBA cations as the templates.

	MFI	MEL(I)	MEL(II)
TPA	−42.27	−17.80	−35.59
TBA	−45.50	−70.51	−45.17

Another important observation is the stronger interaction of TBA with all types of precursors, which would imply that TBA would also induce the formation of MFI. This is obviously not the case and the reason is again the different occupation of the channel intersections. The interaction of TPA in both MEL intersections, even at complete occupation, does not exceed the stabilization by TBA, even though the intersections are only partly occupied in the latter case.

It appears that the difference in action of TPA or TBA becomes relevant in the nanoparticle consisting of 8-Si_{33} structures, because there are several intersections that require stabilization in these systems. Differences between TPA and TBA arise because of the repulsive interactions of the ends of hydrocarbon chains of different lengths.

The question that remains is whether there is a discriminating role for TPA or TBA in the formation of the different types of Si_{33} oligomer formation.

3. Conclusions

The results discussed above show that the zeolite synthesis from Si_{33} precursors is a complex process. The SDA-precursors interactions are very different from the simply lock-and-key model, and the role of template is not simply limited to the scaffolding. From the obtained data, it seems that the importance of SDA also play a role in properly aligning the silica precursors and preventing the hydrolysis by retaining the shape of initial channel formed in the precursors.

We realize that the building units as deducted in the retro-analysis have to be considered idealized. In the real zeolite crystallization system a mixture of many additional oligomers will be present. Also the units that will be associated through the interaction with the templating cation cannot be identical to the Si_{33} units. The essence is the presence of the proper cavities in the silicate complexes when being brought together. We note that according to the building scheme discussed in this paper, monomer species have to be introduced to complete the structures.

There are more factors that can control the selectivity of zeolite structure formation. The assembly processes for MFI and MEL show many similarities with respect to the template location and intermediates. Evidently, the differences in the interaction strength and the way of alignment by both SDAs which seem to be the controlling factor. These factors are the most pronounced in the step of 8-Si_{33} nanoparticle formation, since there are many intersections to be stabilized at the same time. There still remains the question about the role of SDA in the step of Si_{33} formation by TPA and TBA.

Acknowledgement

All simulations have been performed using Discover version 2008.2 by Accelrys Inc. The retro-analysis and visualizations have been done with Zeobuilder version 0.003 [47].

References

[1] D.W. Breck, Zeolite Molecular Sieves: Structure, Chemistry and Use, Wiley and Sons, London, 1974.
[2] R.M. Barrer, Zeolite and Clay Minerals as Sorbents and Molecular Sieves, Academic Press, London, 1978.
[3] R.M. Barrer, Hydrothermal Chemistry of Zeolites, Academic Press, London, 1982.
[4] R. Szostak, Molecular Sieves: Principles of Synthesis and Identification, Van Nostrand Reinhold, New York, 1989.
[5] M.E. Davis, R.F. Lobo, Chem. Mater. 4 (1992) 756–768.
[6] M.E. Davis, Nature 417 (2002) 813–821.
[7] S.I. Zones, in: J. Cejka (Ed.), Proceeding of the 3rd International Zeolite Symposium, Studies in Surface Science and Catalysis Series, Elsevier Science, Amsterdam, 2005, pp. 1–10.
[8] A. Jackowski, S.I. Zones, S.-J. Hwang, A.W. Burton, J. Am. Chem. Soc. 131 (2009) 1092–1100.
[9] S. Yang, A. Navrotsky, Chem. Mater. 14 (2002) 2803–2811.
[10] R.M. Barrer, P.J. Denny, J. Chem. Soc. (1961) 971–982.
[11] Ch. Baerlocher, W.M. Meier, Helv. Chim. Acta 52 (1969) 1853–1860.
[12] E.M. Flanigen, J.M. Bennett, R.W. Grose, J.P. Cohen, R.L. Patton, R.L. Kirchner, J.V. Smith, Nature 271 (1978) 512–516.
[13] C.S. Cundy, P.A. Cox, Micropor. Mesopor. Mater. 82 (2005) 1–78.
[14] B.M. Lok, T.R. Cannan, C.A. Messina, Zeolites 3 (1983) 282–291.
[15] E. Moretti, S. Contessa, M. Padovan, Chim. Ind. 67 (1985) 21.
[16] D.W. Lewis, D.J. Willock, C.R.A. Catlow, J.M. Thomas, G.J. Hutchings, Nature 382 (1996) 604–606.
[17] D.W. Lewis, C.M. Freeman, C.R.A. Catlow, J. Phys. Chem. 99 (1995) 11194–11202.
[18] B.M. Szyja, A.P.J. Jansen, T. Verstraelen, R.A. van Santen, Phys. Chem. Chem. Phys. 11 (2009) 7605–7610.
[19] L. Gómez-Hortigüela, J. Pérez-Pariente, F. Corà, Chem. Eur. J. 15 (2009) 1478–1490.
[20] L. Gómez-Hortigüela, A.B. Pinar, J. Pérez-Pariente, F. Corà, Chem. Mater. 21 (2009) 3447–3457.
[21] R. Ravishankar, C.E.A. Kirschhock, B.J. Schoeman, P. Vanoppen, P.J. Grobet, S. Storck, W.F. Maier, J.A. Martens, F.C. De Schryver, P.A. Jacobs, J. Phys. Chem. B 102 (1998) 2633–2639.
[22] C.S. Cundy, J.O. Forrest, R.J. Plaisted, Micropor. Mesopor. Mater. 66 (2003) 143–156.
[23] J.M. Fedeyko, J.D. Rimer, R.F. Lobo, D.G. Vlachos, J. Phys. Chem. B 108 (2004) 12271–12275.
[24] J.H. van der Waals, J.C. Platteeuw, Adv. Chem. Phys. 2 (1959) 1–57.
[25] E.J.P. Feijen, K. De Vadder, M.H. Bosschaerts, J.L. Lievens, J.A. Martens, P.J. Grobet, P.A. Jacobs, J. Am. Chem. Soc. 116 (1994) 2950–2957.
[26] S. Oliver, A. Kuperman, G.A. Ozin, Angew. Chem. Int. Ed. 37 (1998) 46–62.
[27] C.E.A. Kirschhock, R. Ravishankar, F. Verspeurt, P.J. Grobet, P.A. Jacobs, J.A. Martens, J. Phys. Chem. B 103 (1999) 4965–4971.
[28] C.E.A. Kirschhock, V. Buschmann, S. Kremer, R. Ravishankar, C.J.Y. Houssin, B.L. Mojet, R.A. van Santen, P.J. Grobet, P.A. Jacobs, J.A. Martens, Angew. Chem. Int. Ed. 40 (2001) 2637–2640.
[29] T. Verstraelen, B.M. Szyja, D. Lesthaeghe, R. Declerck, V. Van Speybroeck, M. Waroquier, A.P.J. Jansen, A. Aerts, L.R.A. Follens, J.A. Martens, C.E.A. Kirschhock, R.A. van Santen, Top. Catal. 52 (2009) 1261–1271.
[30] M.W. Anderson, J.R. Agger, J.T. Thornton, N. Forsyth, Angew. Chem. Int. Ed. 35 (1996) 1210–1213.
[31] R. Brent, M.W. Anderson, Angew. Chem. Int. Ed. 47 (2008) 5327–5330.
[32] B.B. Schaack, W. Schrader, F. Schüth, Angew. Chem. 120 (2008) 9232–9235.
[33] F. Schüth, Curr. Opin. Solid State Mater. Sci. 5 (2001) 389–395.
[34] B.J. Schoeman, Micropor. Mesopor. Mater. 22 (1998) 9–22.
[35] P.-P.E.A. de Moor, T.P.M. Beelen, B.U. Komanschek, O. Diat, R.A. van Santen, J. Phys. Chem. B 101 (1997) 11077–11086.
[36] T.M. Davis, T.O. Drews, H. Ramanan, C. He, J. Dong, H. Schnablegger, M.A. Katsoulakis, E. Kokkoli, A.V. McCormick, R. Lee Penn, M. Tsapatsis, Nat. Mater. 5 (2006) 400–408.
[37] P.C. Magusin, V.E. Zorin, A. Aerts, C.J. Houssin, A.L. Yakovlev, C.E.A. Kirschhock, J.A. Martens, R.A. van Santen, J. Phys. Chem. B 109 (2005) 22767–22774.
[38] P.-P.E.A. DeMoor, T.P.M. Beelen, R.A. van Santen, L. Beck, M.E. Davis, J. Phys. Chem. B 104 (2000) 7600–7611.
[39] A.V. Goretsky, L.W. Beck, S.I. Zones, M.E. Davis, Micropor. Mesopor. Mater. 28 (1999) 387–393.
[40] E. de Vos Burchart, H. van Koningsveld, B. van de Graaf, Micropor. Mater. 8 (1997) 215–222.
[41] J.C.G. Pereira, C.R.A. Catlow, G.D. Price, J. Phys. Chem. A 103 (1999) 3252–3267.
[42] P. Dauber-Osguthorpe, V.A. Roberts, D.J. Osguthorpe, J. Wolff, M. Genest, A.T. Hagler, Proteins Struct. Funct. Genet. 4 (1988) 31–47.
[43] J. Maple, U. Dinur, A.T. Hagler, Proc. Natl. Acad. Sci. U.S.A. 85 (1988) 5350–5354.
[44] E.C. Molloy, R.T. Cygan, F. Bonhomme, D.M. Teter, A. Navrotsky, Chem. Mater. 16 (2004) 2121–2133.
[45] J.J. Williams, C.W. Smith, K.E. Evans, Z.A.D. Lethbridge, R.I. Walton, Chem. Mater. 19 (2007) 2423–2434.
[46] R. Garcia, E.F. Philp, A.M.Z. Slavin, P.A. Wright, P.A. Cox, J. Mater. Chem. 11 (2001) 1421–1425.
[47] T. Verstraelen, V. Van Speybroeck, M. Waroquier, J. Chem. Inf. Model. 48 (2008) 1530–1541.